Self-Association Energetics of an Intact, Full-Length Nuclear Receptor: The B-Isoform of Human Progesterone Receptor Dimerizes in the Micromolar Range†

Aaron F. Heneghan, Nancy Berton, Michael T. Miura, and David L. Bain*

Department of Pharmaceutical Sciences, University of Colorado Health Sciences Center, Denver, Colorado 80262

Received April 1, 2005; Revised Manuscript Received May 10, 2005

ABSTRACT: We are focused on understanding the mechanisms underlying eukaryotic gene regulation, using the human progesterone receptor (PR) and its interactions with its DNA response elements as a model system. An understanding of PR function is complicated by the presence of two transcriptionally distinct isoforms, an 83 kDa A-receptor (PR-A) and a 99 kDa B-receptor (PR-B). The two isoforms are identical except the B-receptor contains an additional 164 residues at its N-terminus. As a first step toward understanding the principles by which the two isoforms assemble at complex promoters, we examined the energetics of PR-B self-association using sedimentation velocity and sedimentation equilibrium methods. Full-length human PR-B was purified to 95% homogeneity from baculovirus-infected insect cells. Using a fluorescence hormone binding assay, we determined the purified protein to be highly active in its ability to bind ligand. Sedimentation velocity studies of hormone-bound PR-B at pH 8.0, 4 °C, and 50 mM NaCl demonstrate that it undergoes a concentration-dependent change in its sedimentation coefficient, existing as a 4.0S species at submicromolar concentrations but forming a 5.7S species at higher concentrations. These results strongly suggest that PR-B undergoes self-association in the micromolar range. This hypothesis was examined rigorously using sedimentation equilibrium. Global analysis of the sedimentation equilibrium data demonstrated that PR-B self-association was well described by a monomer−dimer model with a dimerization free energy of -7.2 ± 0.7 kcal/mol. The role of NaCl in regulating PR-B dimerization was examined by carrying out sedimentation velocity and equilibrium studies under high salt conditions. At 300 mM NaCl, PR-B is exclusively monomeric in the micromolar range, thus revealing a significant ionic contribution to the assembly energetics. Further, the monomer sediments as a structurally homogeneous, but highly asymmetric, 4.0S species. Limited proteolysis of PR-B demonstrated that the hydrodynamic asymmetry is due in part to an extended, nonglobular conformation localized to the N-terminal region of PR-B. In contrast, the DNA binding domain (DBD) and hormone binding domain (HBD) exist as independent structural units, and the activation function N-terminal to the DBD (AF-1) shows moderate structure. These results represent the first rigorous analysis of the self-assembly energetics of an intact nuclear receptor and suggest that PR function is more complex than envisioned by traditional models.

Progesterone receptors (PR)[1] are members of the nuclear receptor superfamily of ligand-activated transcription factors (*1*). An understanding of PR function is complicated by the fact that the receptors exist as two functionally distinct isoforms: an 83 kDa A-receptor (PR-A) and a 99 kDa B-receptor (PR-B). The two proteins are identical except for a 164 amino acid extension at the N-terminus of PR-B (see Figure 1). Both isoforms are characterized by a centrally located DNA binding domain (DBD) and a C-terminal hormone binding domain (HBD). The two domains are linked by a 50 amino acid "hinge" sequence of unclear function. Transcriptional activation functions are located N-terminal to the DBD (AF-1) and within the HBD (AF-2). The 164-residue B-unique sequence (BUS) contains a context-dependent transcriptional activation function, AF-3 (*2*). Despite their near sequence identity, the two isoforms display dramatically different functional properties on natural and synthetic promoters. PR-B is typically a much stronger transcriptional activator than PR-A (*3*). The antiprogestin RU486 acts as a partial agonist toward the B-receptor though it is a pure antagonist toward the A-receptor (*4*). PR-A "knockout" mice develop uterine dysplasia and abnormal ovaries (*5*), while PR-B gene knockouts affect the mammary glands, causing premature ductal growth arrest and incomplete lobular−alveolar differentiation (*6*). Microarray studies have revealed that PR-A and PR-B regulate different subsets of genes (*7*). At the clinical level, breast cancer patients with high PR-A:PR-B ratios relapse with higher frequency compared to patients with low PR-A:PR-B ratios (*8*). A molecular understanding of PR-A and PR-B functional differences may permit the development of isoform-specific

† This work was supported by NIH Grant RO1-DK061933 to D.L.B. and by the Tissue Culture Core Laboratory of the Cancer Center of the University of Colorado Health Sciences Center.

* To whom correspondence should be addressed. Phone: 303-315-1416. Fax: 303-315-0274. E-mail: david.bain@uchsc.edu.

[1] Abbreviations: PR, progesterone receptor; PR-A, progesterone receptor A-isoform; PR-B, progesterone receptor B-isoform; HBD, hormone binding domain; DBD, DNA binding domain; BUS, B-unique sequence; AF, activation function; PAGE, polyacrylamide gel electrophoresis; PRE, progesterone response element; DTT, dithiothreitol.

10.1021/bi050609i CCC: $30.25
Published on Web 06/17/2005

ligands and thus more targeted treatments for hormone-dependent diseases such as breast or endometrial cancer.

PR and other steroid receptors (androgen receptor, glucocorticoid receptor, estrogen receptor, and mineralocorticoid receptor) are thought to activate transcription through a multistep reaction pathway beginning with binding of their respective hormone in the cytosol, release of heat shock proteins, and dimerization of the receptor (*1*). Dimerization is thought to be mediated through the C-terminal hormone binding domain. Traditional models then propose that the ligand-bound receptor is translocated into the nucleus, binds its hormone response elements at upstream promoter sites, and recruits an array of coactivating proteins capable of remodeling chromatin and interacting with the basal transcriptional machinery (*9*, *10*). A key aspect of transcriptional activation, however, remains the initial solution dimerization of the hormone-bound receptor. Indeed, solution dimerization of steroid receptors is taken to be a compulsory step in transcriptional activation (*1*).

Exactly why PR and other steroid receptors undergo solution assembly is not entirely clear. Generally speaking, self-association serves to regulate the population of the active DNA binding species (e.g., dimer), thus regulating transcriptional activation. This interpretation derives from classic studies of DNA binding proteins such as bacteriophage λ repressor and *trp* repressor that demonstrated a thermodynamic linkage between protein self-assembly and high-affinity dimer binding to palindromic operator sites (*11*, *12*). Consistent with this, early studies of the estrogen receptor revealed that removal of sequences responsible for solution dimerization resulted in extremely weak binding to its palindromic response elements and significant loss of transcriptional activity (*13*). The importance of a preformed dimer was reinforced by studies indicating that glucocorticoid receptor dimer formation was a rate-limiting step in GRE binding (*14*). Work on progesterone receptors also indicated that dimers formed in solution (*15*) and that only the dimer species was competent to bind DNA (*16*). However, later studies on PR demonstrated that binding activity did not necessarily require prior dimerization (*17*), that PR dimerization and DNA binding affinity were not significantly influenced by ligand (*18*, *19*), and that PR could regulate genes in the absence of its hormone, progesterone (*20*, *21*). Moreover, naturally occurring PR-regulated promoters appear not to contain an abundance of symmetric palindromic PREs but rather are comprised of clusters of half-site PREs (B. M. Jacobsen and K. B. Horwitz, personal communication). Finally, recent studies demonstrate that steroid receptor-mediated gene regulation is highly dynamic, involving ordered and cyclical "hit and run" interactions with upward of 50 different proteins (*22*, *23*). Taken together, these studies suggest that the complexity of eukaryotic gene regulation may require PR dimers (and possibly monomers) to play functional roles other than simply acting as a high-affinity DNA binding species.

To better understand the role of solution dimerization in PR isoform-mediated gene regulation, we have conducted a quantitative analysis of PR-B self-association energetics. The work presented here represents the first rigorous study of the self-assembly properties for a full-length nuclear receptor and demonstrates that PR-B self-association is significantly less favorable than the typical nanomolar affinity estimated for related estrogen and glucocorticoid receptors. As a result, these studies raise questions about the relative roles of monomer and dimer in PR-dependent biological function and may additionally offer insight into the mechanisms by which closely related steroid receptors generate transcriptional diversity.

EXPERIMENTAL PROCEDURES

Expression and Purification of Hexahistidine-Tagged Human Progesterone Receptor B (PR-B). An expression vector encoding residues 1−933 of human PR-B fused to an N-terminal hexahistidine sequence was a generous gift of Dr. Dean P. Edwards. Saturating amounts of progesterone were present at all times during purification and storage, and all purification steps were carried out at 4 °C. PR-B was expressed in baculovirus-infected Sf9 insect cells as previously described (*24*). Whole cell extracts were prepared as previously described (*25*). PR-B was first partially purified using Ni^{2+}−agarose chromatography (Qiagen). Loading buffer conditions were 20 mM Tris (pH 8.0 at 4 °C), 10% glycerol (w/v), 500 mM NaCl, 15 mM β-ME, 35 mM imidazole, and 10^{-5} M progesterone. Upon binding PR-B to the Ni^{2+}−agarose column, the resin was extensively washed with loading buffer, and PR-B was eluted with 250 mM imidazole. The PR-B-containing eluate was dialyzed into a buffer containing 20 mM Tris (pH 8.0), 10% glycerol (w/v), 100 mM NaCl, 15 mM β-ME, and 10^{-5} M progesterone and concentrated using SP-Sepharose (Amersham-Pharmacia). After elution with a 300 mM NaCl step gradient, PR-B was loaded directly onto a Sephacryl S-200 size exclusion column equilibrated in 20 mM Tris (pH 8.0), 10% glycerol (w/v), 100 mM NaCl, 15 mM β-ME, and 10^{-5} M progesterone. The fractionated protein was then concentrated using Q-Sepharose, eluted in high salt, flash-frozen, and stored in liquid nitrogen. PR-B was judged to be approximately 95% pure by quantitation of Coomassie Blue-stained SDS−PAGE. PR-B concentration was determined using a calculated extinction coefficient of 65020 M^{-1} cm^{-1} (*26*). Experimental determination of the extinction coefficient using the method of Edelhoch (*27*, *28*) resolved a value within 5% of the calculated value (data not shown). Typical yields were 1−2 mg of pure PR-B/L of culture.

Preparation of Apoprotein and Determination of PR-B Hormone Binding Activity. PR-B bound with progesterone was dialyzed overnight (at least 15 h) at 4 °C against 20 mM Tris, pH 8.0 (titrated at 4 °C), 10% (w/v) glycerol, 100 mM NaCl, 1 mM DTT, and 0.05% Tween-20. After dialysis, 20 μL aliquots of the dialyzed protein were injected onto a C_{18} reverse-phase HPLC column (0.25 × 25 cm; Vydac). The column was developed using a 0−55% acetonitrile gradient in the presence of 0.1% H_3PO_4 in water. A dual wavelength detector (Waters) was used to monitor products. Integration of the eluted peaks was used to determine total progesterone concentrations remaining in the dialysis sample (i.e., progesterone still bound to PR-B and free progesterone present in the dialysis membrane). Progesterone concentrations were determined via a standard curve, generated by injecting known concentrations of progesterone onto the HPLC column.

For fluorescence studies, the dialyzed apoprotein was diluted into the above dialysis buffer to a concentration of

0.5 μM. RU486 (Sigma) was dissolved in ethanol and the concentration determined by UV absorbance. All data were collected at 4 °C with a nitrogen flow around the cell to prevent condensation. Data were collected with an Aviv automated titrating differential/titrating ATF104 spectrofluorometer. To minimize photobleaching from the high-intensity lamp, the excitation bandwidth was set at 0.16 nm, and data were averaged at each point for 1 s. The emission bandwidth was set at 6.4 nm. RU486 was incrementally injected into the cuvette covering a range of 0.05 to 5 μM, with the ethanol concentration reaching 2% at the highest concentration. Titration data were collected at 280 nm excitation and 340 nm emission wavelengths. The sample was stirred in the dark during the 5 min necessary to achieve equilibrium upon ligand addition. Preceding and after each titration experiment, an excitation spectrum at 340 nm emission wavelength and emission spectra at 295, 280, and 260 nm excitation wavelengths were obtained to ensure the spectra were consistent between runs. All data were corrected for dark current, photobleaching, dilution, and inner filter effects by standard methods (*29*).

Sedimentation Velocity. Sedimentation was carried out on a Beckman XL-A analytical ultracentrifuge equipped with absorbance optics, using a two-channel Epon centerpiece and an An-60 rotor. PR-B at a series of concentrations ranging from 2 to 0.25 μM was sedimented at 4 °C in a buffer containing 20 mM Hepes, pH 8.0, 2.5 mM $MgCl_2$, 1 mM DTT, 1 mM $CaCl_2$, and 10^{-5} M progesterone and either 50 mM NaCl (low salt buffer) or 300 mM NaCl (high salt buffer). The rotor speed for all experiments was 50000 rpm with scans taken as quickly as the ultracentrifuge would allow, typically every 4 min with the absorbance monitored at 230 nm. The sedimentation coefficient distribution, $g(s^*)$, was calculated using the program DCDT+ (*30*). The $g(s^*)$ distribution was corrected to 20 °C and water ($s_{20,w}$) using standard methods (*31*). Under conditions where s could be assigned to a discrete assembly state (e.g., monomer), the frictional coefficient (f) was calculated using the Svedberg equation

$$s_{20,w} = M(1 - \nu\rho)/Nf \quad (1)$$

where M is the molecular weight, ν is the partial specific volume of the protein, ρ is the solvent density, and N is Avogadro's number. The frictional coefficient of a sphere of the same molecular weight, f_0, was calculated assuming a degree of hydration of 0.3 g of water/g of protein (*32*, *33*).

Sedimentation Equilibrium. Sedimentation equilibrium was carried out under the identical two buffer conditions as described for the sedimentation velocity experiments. The samples were spun to sedimentation equilibrium on a Beckman XL-A analytical ultracentrifuge using a six-channel Epon centerpiece. Three different protein concentrations were allowed to reach equilibrium at 4 °C in the ratios of approximately 10:5:2.5, with the highest concentration being 0.9 μM. The three concentrations of PR-B were equilibrated at 14000, 18000, and 21000 rpm. Samples were judged to be at equilibrium by successive subtraction of scans. Buffer density was calculated on the basis of the salt composition and the temperature of the buffer (*34*). The partial specific volume for PR-B was calculated by summing the partial specific volumes of each individual amino acid (0.7232 mL/g) (*35*). Data were analyzed using nonlinear least squares (NLLS) parameter estimation as implemented in the program NONLIN (*36*). All data were first analyzed to resolve σ, the reduced molecular weight. Using the equation

$$\sigma = M(1 - \nu\rho)\omega^2/RT \quad (2)$$

the weight average molecular weight, M, was calculated for each initial loading concentration. In this equation, ν is the partial specific volume of the protein, ρ is the solvent density, ω is the angular velocity, R is the gas constant, and T is the absolute temperature in kelvin. The data were also analyzed globally in order to resolve self-association constants using the equation

$$Y_r = \delta + \alpha \exp[\sigma(r^2 - r_0^2)] + \sum \alpha^N K_N \exp[N\sigma(r^2 - r_0^2)] \quad (3)$$

where Y_r is absorbance at radius r, δ is the baseline offset, α is the monomer absorbance at the reference radius, r_0, σ is the reduced molecular weight (eq 2), N is the stoichiometry of the reaction, and K_N is the association constant of the reaction $NM \leftrightarrow M_N$. σ for all fits was set at the value of the monomer calculated by the amino acid composition. Resolved values of K_N were converted from absorbance to molar association constants on the basis of the calculated ϵ_{230} (*37*). Free energies for the assembly reactions (ΔG_N) were calculated using the equation $\Delta G_N = -RT \ln K_N$.

Limited Proteolysis of PR-B. EndoGluC was of sequencing grade obtained from Roche Applied Science. Digestion was carried out using 1 μM PR-B in buffer conditions and temperature identical to the low salt sedimentation studies. Enzyme was added at a PR-B:enzyme mass ratio of 50:1. The reaction was allowed to proceed for 2 h with aliquots taken as a function of time. Reactions were terminated by addition of SDS−PAGE loading dye and boiling of the sample. Aliquots containing 5 μg of PR-B were electrophoresed on 10% SDS−PAGE and either stained with Coomassie Brilliant Blue or transferred to nitrocellulose for immunoblot analysis. The antibodies used for analysis were α266, a polyclonal antibody raised against a peptide corresponding to the DNA binding domain residues V611−C627 [generously donated by Dr. David Toft (*38*)], and C-19, a polyclonal antibody specific for the C-terminal portion of the PR hormone binding domain (Santa Cruz Biotechnology, Inc.).

RESULTS

Quantitative Ligand Binding Analysis Demonstrates That PR-B Is Functionally Homogeneous. Milligram quantities of PR-B (Figure 1a) were purified from baculovirus-infected Sf9 insect cells using four chromatographic steps. SDS−PAGE analysis showed that PR-B was at least 95% pure by densitometric scans of Coomassie Blue-stained gels (Figure 1b). The purified protein was immunoreactive to antibodies specific for the N-terminal hexahistidine sequence and C-terminal HBD sequence, demonstrating that PR-B was not significantly degraded or proteolyzed during purification (data not shown). Finally, though hexahistidine sequences can influence protein function (*39*), our work on PR isoforms

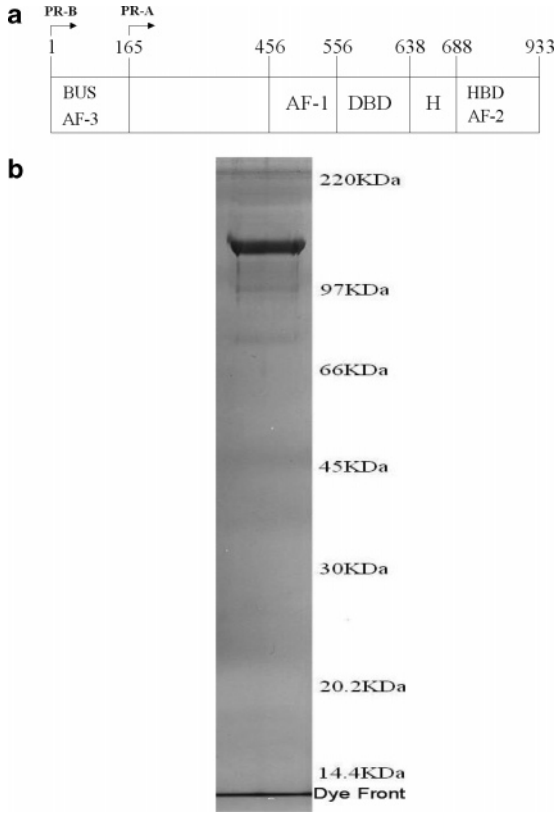

FIGURE 1: Progesterone receptor domain structure and purification of PR-B. (a) Schematic of the primary amino acid sequence for PR-A and PR-B isoforms. Functional regions are as indicated: DBD, DNA binding domain; HBD, hormone binding domain; H, hinge; AF, activation function; BUS, B-unique sequence. PR-B is defined as amino acids 1−933; PR-A is defined as amino acids 165−933. (b) Baculovirus-expressed PR-B was purified as described in Experimental Procedures. The purified protein (5 μg) was resolved by 10% SDS−PAGE and silver-stained. Molecular mass markers are indicated to the right. Densitometric scanning of Coomassie-stained gels indicates PR-B is ~95% pure.

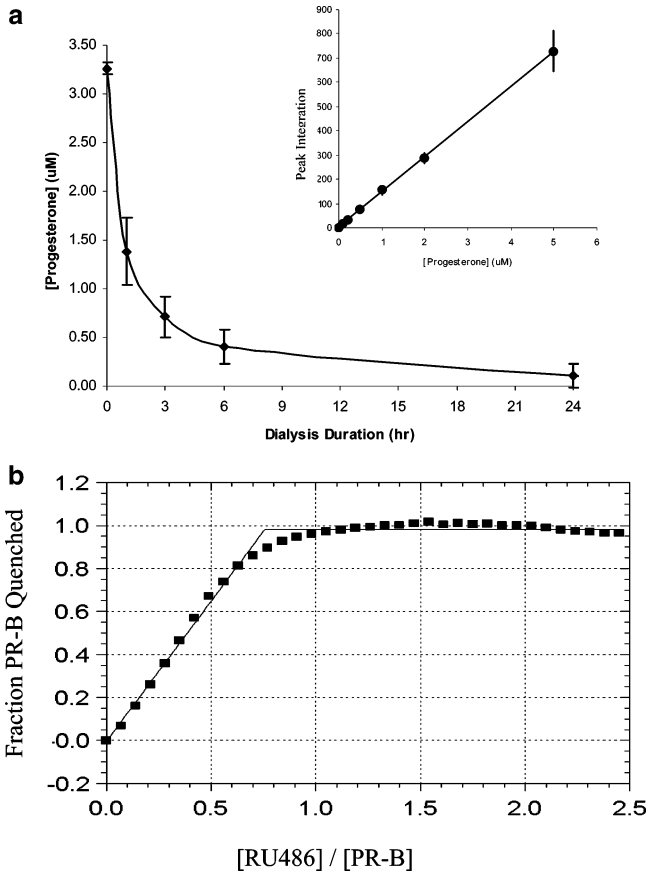

FIGURE 2: Titration of PR-B with the ligand RU486 under stoichiometric binding conditions. (a) HPLC analysis of residual progesterone remaining as a function of PR-B dialysis time. Data points were determined in triplicate; error bars correspond to 1 SD. The solid line represents a phenomenological fit to emphasize the trend in the data. Inset: Standard curve used to determine residual progesterone concentrations. (b) Stoichiometric fluorescence-monitored ligand binding assay to determine fractional activity for PR-B. Data points represent normalized quenching of intrinsic PR-B fluorescence as a function of RU486 concentration. The line represents the best-fit, simultaneous analysis of data fit to a phenomenological breakpoint transition curve. The PR-B concentration was 0.5 μM.

lacking only the HBD demonstrated that the sequence had no effect on receptor properties (*40*, *41*).

Though SDS−PAGE analysis demonstrates that PR-B is highly pure, it does not address whether PR-B is functionally homogeneous. That is, what fraction of the PR-B population is competent to bind ligand? The fractional activity of PR-B was determined using a quantitative ligand binding assay. Traditional studies of nuclear receptor−ligand interactions have used the charcoal adsorption assay. While unparalleled for the semiquantitative analysis of impure protein, the charcoal assay has long been known to have serious limitations when used to quantitatively analyze highly purified receptor preparations (*42*). More recently, studies that directly compared the charcoal assay to quantitative approaches confirmed this limitation (*43*). In light of this concern, we have used the intrinsic fluorescence of PR-B and the ability of the antiprogestin, RU486, to quench this fluorescence in order to assess PR-B fractional ligand binding activity.

Because PR-B was purified and stored in progesterone, it was necessary to demonstrate that the ligand was removed prior to conducting the ligand binding assay. Toward this end, PR-B was extensively dialyzed against a buffer containing no progesterone (see Experimental Procedures). The extent of total progesterone remaining within the dialysis membrane (i.e., progesterone still bound to PR-B and free progesterone) was determined by reverse-phase HPLC. Figure 2a shows the result of residual progesterone concentration determined as a function of PR-B dialysis time. It is evident that greater than 90% of ligand is removed after approximately 15 h of dialysis and falls below the limit of detection by 24 h. It should be noted that the apparent rate of progesterone loss reflects the off-rate for PR-B−progesterone dissociation, the diffusion rate of progesterone, and the rate at which progesterone crosses the dialysis membrane.

The functional activity of PR-B was determined using a fluorescence-based ligand binding assay. Upon generating ligand-free receptor, RU486 was incrementally added to PR-B under stoichiometric binding conditions (Figure 2b). RU486 was chosen as a ligand due its ability to generate a more significant change in PR-B intrinsic fluorescence compared to the natural agonist, progesterone. This difference is likely due to the different binding orientations of the two ligands and their differential effects on PR structure (*44*−*46*). Because the protein concentration was micromolar, well above the nanomolar binding affinity of RU486 (*47*), the change in fluorescence signal represents the stoichiometric

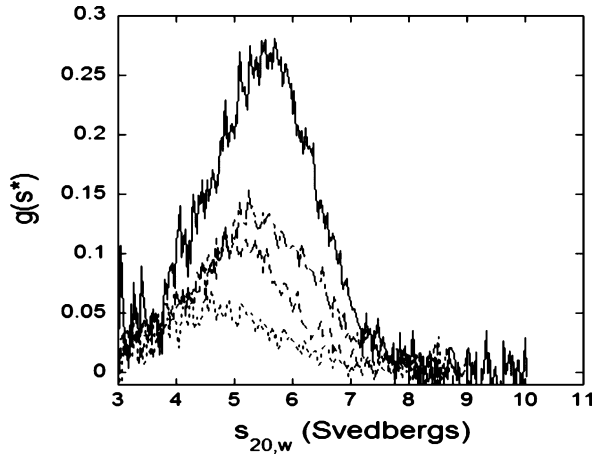

FIGURE 3: Concentration dependence of $g(s^*)$ distribution for PR-B at pH 8.0, 50 mM NaCl, and 4 °C. Initial loading concentrations were 2 μM (solid line), 1 μM (long dashed line), 0.5 μM (medium dashed line), and 0.2 μM (short dashed line). $g(s^*)$ distributions were determined by analysis of successive scans taken at each loading concentration. Peak $g(s^*)$ values correspond to the apparent sedimentation coefficient at each PR-B concentration.

addition of ligand to PR-B. Using the universally accepted 1:1 stoichiometry of ligand to receptor, the breakpoint in the binding curve reflects the fractional binding activity of PR-B. By simultaneously fitting the data to two straight lines, it is evident that the breakpoint for ligand binding occurs at a ligand:protein molar ratio of 0.76 ± 0.1, indicating that PR-B is ~75% active in this experiment. The fractional activity of different receptor preparations varied from 50% to full activity. The extent of ligand binding was independent of NaCl concentration, indicating that the receptor assembly state (see below) does not influence stoichiometric binding activity.

To conclude that the change in PR-B fluorescence was due only to the site-specific binding of RU486, we repeated the titration under denaturing conditions (either 6 M urea or high temperature); in neither case did RU486 induce a change in PR-B fluorescence. Further, there was also no change in fluorescence when PR-B was titrated with dexamethasone, a structurally similar ligand specific for the glucocorticoid receptor. A PR construct lacking the HBD also showed no change in fluorescence when titrated with RU486. Finally, the RU486-induced signal change could be attenuated by subsequent addition of progesterone, indicating that RU486 binding was both specific and reversible.

Sedimentation Velocity Demonstrates That PR-B Undergoes Self-Association. We used analytical ultracentrifugation to determine the hydrodynamic properties and energetics of PR-B self-association. Studies were initially carried out at 50 mM NaCl in order to aid in the interpretation of concurrent PR-B−DNA analyses, necessarily conducted under low salt conditions. Sedimentation velocity was used to examine the hydrodynamic shape and size of PR-B in solution as a function of protein concentration. Figure 3 shows the sedimentation coefficient distribution $g(s^*)$ determined for four initial protein loading concentrations. Each distribution was calculated using DCDT+ analysis (*30*) to determine the sedimentation coefficient distribution at each initial loading concentration. These data were collected in a buffer containing 20 mM Hepes, pH 8.0, 50 mM NaCl, 2.5 mM $MgCl_2$, 1 mM DTT, 1 mM $CaCl_2$, and 10^{-5} M

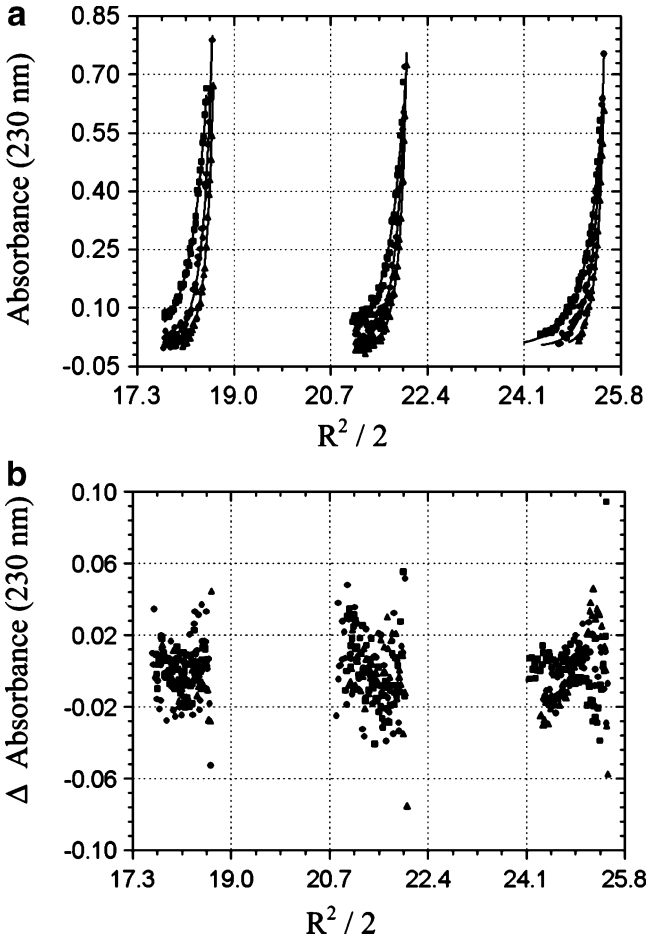

FIGURE 4: Sedimentation equilibrium analysis of PR-B at pH 8.0, 50 mM NaCl, and 4 °C, plotted as absorbance versus $R^2/2$. (a) Initial loading concentrations: 0.9 μM (left), 0.45 μM (center), and 0.23 μM (right). Symbols represent PR-B absorbance at 14000 (squares), 18000 (circles), and 21000 rpm (triangles). Solid lines represent the best-fit model (monomer−dimer) from simultaneous analysis of all nine data sets. The square root of the variance was 0.015 absorbance unit. (b) Residuals from the monomer−dimer equilibrium model plotted as change in absorbance vs $R^2/2$.

progesterone. Sedimentation velocity experiments at four different initial PR-B loading concentrations, 2, 1, 0.5, and 0.25 μM, are shown in Figure 3. Under these conditions, the temperature and buffer corrected distribution shifts from a peak sedimentation coefficient of 5.7 S at higher PR-B concentrations (>1 μM) to a value approaching 4.0 S at lower PR-B concentrations (0.2 μM). (Not shown are rapidly sedimenting species that appear when PR-B concentrations approach 2 μM. These species likely correspond to polydisperse aggregates, suggesting that 2 μM PR-B is near the solubility limit under these conditions.) Concentration dependence to the sedimentation coefficient is diagnostic for a system undergoing self-association. Using complementary sedimentation equilibrium techniques, we addressed the nature of this self-association at 50 mM NaCl.

Sedimentation Equilibrium Demonstrates That PR-B Self-Association Undergoes Monomer−Dimer Equilibrium. Figure 4a shows the results of a series of nine sedimentation equilibrium experiments, carried out in the same buffer conditions as described for the sedimentation velocity experiments. These data consist of three initial loading concentrations in the approximate ratio of 10:5:2.5, with the highest loading concentration of 0.9 μM, well below the

PR-B solubility limit. Each sample was allowed to reach equilibrium at three rotor speeds (14000, 18000, and 21000 rpm). Attempts to globally fit the data to a single species model (i.e., monomer) resulted in a poor quality fit, corresponding to a square root of the variance of 0.022 absorbance units. In contrast, simultaneous analysis of all nine data sets was well described by a monomer−dimer model and a square root of the variance of 0.015 absorbance units. This model resolved a free energy of dimerization equal to -7.2 ± 0.7 kcal/mol, corresponding to a dimerization constant of 1.7 μM at 4 °C. Shown in Figure 4b are the residuals for the global fit. These results are consistent with the sedimentation velocity studies that demonstrated a concentration-dependent change of the sedimentation coefficient in the micromolar range. Attempts to describe the data with more complex models (e.g., monomer−dimer−trimer) did not improve the quality of the fit, allowing us to accept the monomer−dimer model as most appropriate. Finally, the sedimentation equilibrium and velocity results were independent of ligand binding activity (Figure 2), suggesting that loss of binding activity may be due to only localized changes in structure (e.g., amino acid modification or deletion) rather than large-scale unfolding events.

Increased Salt Concentration Decreases PR-B Dimerization and Reveals That the PR-B Monomer Is Structurally Homogeneous. At 50 mM NaCl, PR-B undergoes monomer−dimer assembly in the micromolar range. Thus the peak sedimentation coefficient values seen in Figure 3 do not correspond to any discrete species in solution. Rather, each peak value is a composite average representing both the monomer and the dimer. To assign a more detailed molecular interpretation to the sedimentation coefficient values, we carried out sedimentation equilibrium studies at 300 mM NaCl. Global analysis of all nine data sets resolved a molecular mass of 93436 ± 3224 Da, with a square root of the variance of 0.011 absorbance units (data not shown). The resolved molecular mass is in good agreement with the calculated molecular mass of the monomer, 98995 Da (*48*). The quality of the fit could not be improved by adding additional parameters, such as a dimer component. This result thus demonstrates that, at 300 mM NaCl, PR-B is purely monomeric in the micromolar range. Further, taken together with the 50 mM results, these studies demonstrate that PR-B self-association energetics are governed by a strong ionic component. A thermodynamic analysis of the salt dependence (and hormone dependence) of PR-B self-association is currently underway.

To assess the structural properties of the monomer under these conditions, we carried out a sedimentation velocity analysis of PR-B at the highest concentration used in the sedimentation equilibrium studies. The results of the DCDT+ analysis are plotted in Figure 5. Under these conditions, PR-B sediments with a narrow distribution and a peak value of 4.0 S. Direct fitting of the $g(s^*)$ data resolved a molecular mass of 91236 ± 4234 Da, consistent with the molecular mass of the monomer. The close agreement in molecular masses determined by the two techniques demonstrates that the PR-B monomer is hydrodynamically homogeneous under these conditions. Since the sedimentation equilibrium and velocity results equally underestimate the PR-B molecular mass, it may be that the actual partial specific volume of the protein is slightly higher than calculated, likely due to

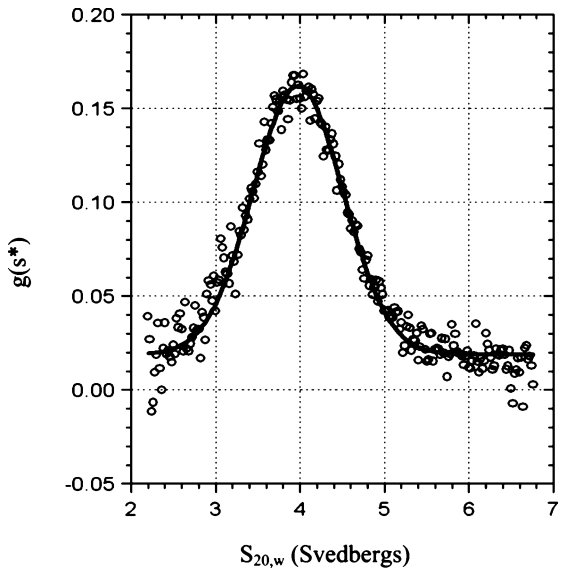

FIGURE 5: $g(s^*)$ distribution for PR-B at pH 8.0, 300 mM NaCl, and 4 °C. Open circles represent $g(s^*)$ distribution at an initial PR-B loading concentration of 0.9 μM. The distribution was determined by global analysis of successive scans. The peak $g(s^*)$ value corresponds to the apparent sedimentation coefficient. The solid line represents the best fit to a single Gaussian curve.

Table 1: Hydrodynamic Properties of the PR-B Monomer Determined by Analytical Ultracentrifugation at pH 8.0, 300 mM NaCl, and 4 °C

S	4.0
f (g/s)	1.14×10^{-8}
f/f_0	1.42
Stokes radius (Å)	64
axial ratio	8:1
M_w (Da)[a]	93436 ± 3224
M_w (Da)[b]	91236 ± 4234

[a] Determined by sedimentation equilibrium. [b] Determined by sedimentation velocity.

posttranslational phosphorylation events (*24*, *49*). Using the Svedberg equation (eq 1) and the monomer molecular mass, we can calculate a frictional coefficient (f) of 1.14×10^{-8} g/s. Comparison of the frictional coefficient to that of a sphere with the same molecular mass (f_0) indicates that PR-B is highly asymmetric with a frictional ratio (f/f_0) of 1.42. Modeling of PR-B as a hydrated prolate ellipsoid yields a ratio of major to minor axes of ~8:1 and a Stokes radius of 64 Å. Table 1 lists all hydrodynamic properties for PR-B at 300 mM NaCl.

Limited Proteolysis Studies of PR-B Support a Nonglobular Conformation. To probe the structural implications of the PR-B asymmetry, we carried out limited proteolysis studies under conditions identical to those of the low salt sedimentation studies. Figure 6 shows an EndoGluC time course digestion of PR-B. It is evident that, in the first 30 min, PR-B is degraded from a full-length protein to three relatively stable fragments with apparent molecular masses of 55, 48, and 45 kDa (labeled as bands 1, 2, and 3 in panel A). Immunoblot analysis (panel B) using antibodies specific to the DBD and HBD demonstrates that each fragment contains both domains. On the basis of approximate molecular masses of 10 kDa for the isolated DBD and 29 kDa for the isolated HBD, these fragments must additionally contain some or all of the N-terminal AF-1 sequence (as diagramed

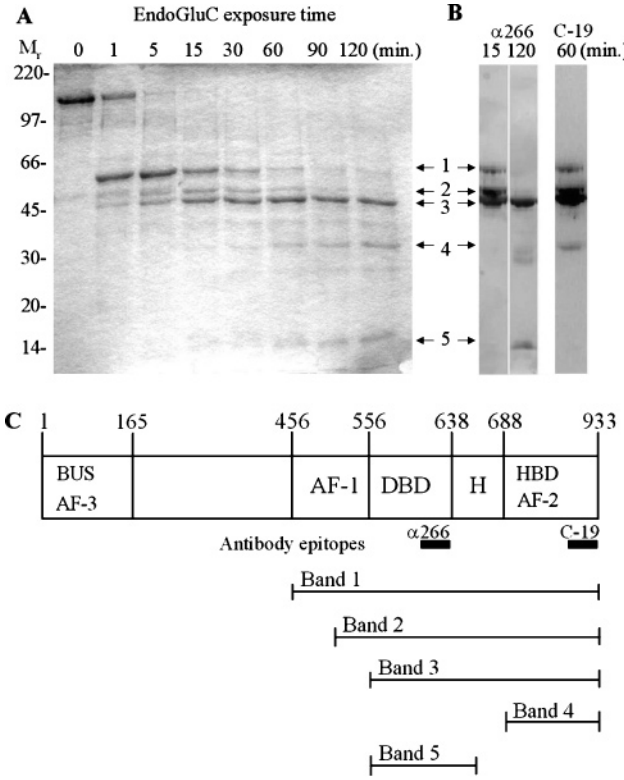

FIGURE 6: Time course for EndoGluC digestion of PR-B. (A) Purified PR-B was digested with EndoGluC for 0−120 min at pH 8.0, 50 mM NaCl, and 4 °C. Resultant peptides were resolved and visualized using Coomassie-stained SDS−PAGE. Major digestion products are indicated by arrows. Molecular weight markers are indicated to the left. (B) Peptides were also probed by immunoblot analysis using antibodies specific to either the DBD (α266) or HBD (C-19). (C) Schematic of intact PR-B structure and PR-B digestion products estimated by apparent molecular weight.

in panel C). Extended exposure to protease generates two additional fragments with apparent molecular masses of 31 and 14 kDa (bands 4 and 5, respectively). These fragments correspond to the isolated DNA binding and hormone binding domains, respectively (see panels B and C). Of note is the complete absence of intermediate fragments generated between the full-length PR-B and the AF1-DBD-HDB species (bands 1, 2, and 3). This result strongly suggests that the ~50 kDa polypeptide sequence N-terminal to AF-1 is largely unstructured and/or in an extended conformation, entirely consistent with the hydrodynamic asymmetry seen in the sedimentation velocity studies. The enhanced proteolysis of the N-terminal region may also be due to noncanonical peptide bond conformations, though this interpretation does not explain the strong asymmetry observed in the sedimentation velocity results. Finally, these results confirm early biochemical characterizations of PR that led to the conclusion that it contained only two independent structural units, the DNA binding domain and hormone binding domain (*1*).

DISCUSSION

Energetics of PR-B Self-Assembly. For many transcription factors, there is a significant thermodynamic linkage between self-assembly and DNA binding (*50*). For example, estrogen receptor solution dimerization is clearly prerequisite to high-affinity binding at its DNA response elements (*13*). In the absence of an explicit determination of the solution dimerization constant, the analysis of protein−DNA binding isotherms resolves only apparent binding constants, which provide only minimal information for understanding DNA binding mechanisms. Further, direct analysis of solution assembly properties provides quantitative insight into the physical and chemical forces that drive oligomerization. Using sedimentation velocity, we demonstrate that, at pH 8.0, 50 mM NaCl, and 4 °C, liganded PR-B undergoes a concentration-dependent change in its average sedimentation coefficient (Figure 3). Sedimentation equilibrium studies carried out under identical conditions demonstrate that this change is due to rapid and reversible monomer−dimer assembly. Global analysis of the equilibrium data resolved a dimerization free energy of −7.2 kcal/mol, equivalent to a dissociation constant of 1.7×10^{-6} M (Figure 4). This relatively weak dimerization constant, determined in the presence of progesterone, is entirely consistent with crystallographic studies indicating that the PR−HBD dimer maintains a small dimerization interface of only 700 Å^2 (*51*). By comparison, the estrogen receptor dimer, thought to dissociate to monomers only in the nanomolar to subnanomolar range (*52*), has a much more extensive dimerization interface of approximately 1700 Å^2 (*53*).

The resolved energetics are also in qualitative agreement with early biochemical analyses of PR self-association (*18*). Using partially purified, calf uterine receptor preparations, Skafar demonstrated that the differential DNA binding properties of estrogen receptors versus progesterone receptors were due to a difference in their self-assembly properties: Estrogen receptor was estimated to dimerize with a dissociation constant of 0.3 nM, while PR was estimated at 7 nM. Contaminating proteins, different solution conditions, and semiquantitative techniques make it difficult to directly compare these earlier studies with our results. Nonetheless, it is clear that even though PR dimers can form in solution (*15*, *19*), PR dimerization affinity is considerably weaker than that of the more stable estrogen receptor.

Finally, in light of the observed self-association energetics for the full-length progesterone receptor, it is worth noting the absence of assembly for any isolated PR domain: Highly purified PR constructs lacking the HBD are quantitatively monomeric over a wide range of conditions and concentrations (*40*, *41*). Likewise, highly purified HBD was found to be entirely monomeric in solution (*51*). These observations suggest that PR-B dimerization is a system or global property of PR-B rather than a "part" property attributable only to the HBD (*1*). This result is presumably due to allosteric contributions from other PR-B regions and domains, even if the HBD provides the sole dimerization interface in solution.

Hydrodynamics of PR-B Self-Assembly. Because the sedimentation coefficient distributions at 50 mM NaCl reflect both monomers and dimers in solution (Figure 3), the peak sedimentation coefficient values at each protein concentration do not correspond to any discrete species. For example, the 5.7S species seen at 2 μM PR-B concentration reflects a near 1:1 ratio of monomer to dimer, based on the dissociation constant of 1.7 μM. However, sedimentation velocity experiments carried out at 300 mM NaCl demonstrate the presence of only a 4.0S species (Figure 5), and the sedimentation equilibrium results demonstrate that this species corresponds to the PR-B monomer. Moreover, direct fitting of the

sedimentation velocity $g(s^*)$ results resolved a molecular mass of 91236 ± 4234 Da, in close agreement to the 93436 ± 3224 Da value determined by sedimentation equilibrium. This concordance demonstrates that under these conditions the PR-B monomer is structurally homogeneous (*30*) and thus affords us insight into the molecular properties of PR-B. For example, the observed asymmetry of the monomer (as measured by a frictional coefficient of 1.42) must be due to either a literal nonspherical PR-B structure (e.g., rodlike), a natively unfolded or partially disordered conformation, or a significantly increased hydration shell; each possibility would lead to an increased apparent volume and thus increased frictional resistance during sedimentation. Limited proteolysis (Figure 6) supports the second hypothesis, demonstrating that residues N-terminal to AF-1 are highly susceptible to proteolytic attack, most likely because they exist in an extended, partially disordered ensemble of conformations. The proteolysis results are also qualitatively similar to previous proteolytic studies carried out on PR isoforms lacking the HBD (*40*, *41*), thus indicating that the HBD does not have an obvious influence on the N-terminal structure. Further, these results confirm that there are only two independent structural units in PR-B (DBD and HBD) and that AF-1 may maintain a degree of stable structure. Finally, the current results make it clear that the PR 4S species long seen by classical glycerol gradient studies is indeed the monomer (*54*).

Salt Dependence to the Assembly Reaction. Since PR-B is exclusively monomeric at 300 mM NaCl, we can estimate a lower limit to the dimerization constant at these conditions. Analysis of the 300 mM sedimentation equilibrium data using a monomer−dimer model (data not shown) suggests that the dimerization dissociation constant under these conditions is minimally 8.1 μM. This value translates into a 5-fold decrease in dimerization affinity compared to the 1.7 μM constant obtained at 50 mM NaCl. The net number of thermodynamic ions released over this range, $\Delta\nu_{NaCl}$ [where $\Delta\nu_{NaCl} = d \ln K_{assoc}/d \alpha_{NaCl}$ (*55*)], corresponds to at least 1.7 ions. Comparison of this result to the crystal structure of the PR HBD leads to the possibility that at least some of the salt effect might be due to attenuation of hydrogen-bonding interactions at the dimer interface (*51*). However, if self-association is indeed a global property of PR-B, it is reasonable to assume that other regions and domains of PR play a role in the observed ionic linkage.

Functional Consequences of a Micromolar Dimerization Constant. The weak dimerization affinity reported here has important implications for the mechanisms of PR-B binding to its DNA response elements. It is commonly accepted that, upon binding ligand, steroid receptors release heat shock proteins, dimerize, interact with their hormone response elements, and recruit coactivating proteins to activate gene expression. However, since the DNA binding affinity of PR-B has typically been measured in the nanomolar range[2] (*56*) and estimates of intracellular receptor concentration put PR in the nanomolar range (*57*), essentially all (~99.9%) of the liganded PR-B in solution would be monomeric, assuming a micromolar dissociation constant. Moreover, since PR dimerization affinity decreases at higher NaCl concentrations (see Results), the proportion of dimers likely becomes infinitesimally small at physiological salt concentrations. Keeping in mind that a nanomolar estimate of intracellular PR concentration can only be taken as a rough guide due to macromolecular compartmentalization and crowding effects, it is nonetheless tempting to speculate that PR-B dimerization does not precede binding to DNA response elements. That is, in vivo, PR monomers only form dimers through a DNA-induced dimerization event. Consistent with this are reports indicating that chicken PR does not require solution dimerization to function (*17*). The possibility that PR-B functions as a monomer may also explain the puzzling fact that, unlike estrogen, progesterone does not act as a strong effector for driving dimerization of its cognate receptor (*19*).

The above hypothesis clearly contradicts the traditional model of steroid receptor function indicating that a preformed dimer is the active DNA binding species (*1*, *15*, *19*). If, however, PR dimers are indeed the only species capable of binding DNA response elements, then the self-assembly energetics presented here make it clear that these molecules must have equilibrium dissociation constants in the picomolar range, given the nanomolar concentrations estimated for total PR in vivo. Though picomolar binding affinities seem unlikely, only pre-steady-state kinetic analyses of PR−PRE interactions will reveal whether the protein binds as a DNA-induced dimer, a preformed dimer, or both.

The micromolar self-association energetics become even more intriguing when compared against estimates of the dimerization constants for other members of the steroid receptor family. Keeping in mind that these estimates were carried out using semiquantitative techniques, isolated domains, or partially purified proteins and under a variety of solution conditions, the results suggest an extraordinary range of dissociation constants accessible to steroid receptors. For example, all estimates of estrogen receptor dimerization put the dissociation constant at nanomolar or subnanomolar (ref *52* and references cited therein). Estimates of glucocorticoid receptor dimer dissociation have ranged from 4 to 20 nM (*58*, *59*). By contrast, androgen receptor has been estimated to dimerize in the high nanomolar to low micromolar range (*60*). (As of yet, there are no data on the self-assembly properties of the final steroid receptor family member, mineralocorticoid receptor.) Only rigorous thermodynamic studies will confirm the accuracy of these estimates; thus one must use caution in making direct comparisons to the present study. However, these results suggest that closely related receptors are capable of covering roughly 4 orders of magnitude in dimerization affinities. We speculate that this range of affinities plays a role in receptor-specific function and diversity. With the exception of the estrogen receptor, all steroid receptors are capable of binding the same minimal hormone response element. It may be possible that the arrangement and affinities for half-sites versus palindromic sites are dictated by the assembly state of the specific steroid receptor. For example, biochemical studies indicate that glucocorticoid receptor binds to individual MMTV half-sites as a dimer (*59*, *61*); the weak dimerization affinity of PR may allow it to bind to MMTV promoter half-sites as a monomer. This differential stoichiometry would add another

[2] Rigorous thermodynamic analysis of PR-B interactions with its DNA response elements under the identical low salt conditions described here confirms an apparent nanomolar binding affinity (A. F. Heneghan, K. Connaghan-Jones, M. T. Miura, and D. L. Bain, manuscript in preparation).

level of control to the regulation of transcriptional activity, perhaps through differential recruitment of coactivating proteins (*10*). It may be then that evolutionary pressure has selected for differential dimerization energetics not only as a means to regulate the concentration of active DNA binding species but further suggests that mechanisms of action for one steroid receptor do not necessarily apply to all family members.

SUMMARY

The results presented here demonstrate that PR-B self-association is significantly weaker than predicted on the basis of traditional models of receptor function. If receptors such as PR-B bind DNA response elements only as preformed dimers, then their intrinsic affinity toward PREs is likely to be in the picomolar range rather than the nanomolar range. Alternatively, if PR-B binds palindromic response elements as a DNA-induced dimer, then this mechanism immediately calls into question the role of solution dimerization and the role of progesterone as a mediator of dimerization. Finally, it is important to point out that the conclusions drawn here could only be reached due to the rigorous and quantitative approach employed; it will be interesting to see what properties other nuclear receptors, in particular steroid receptors, reveal when they are subjected to detailed thermodynamic and kinetic analyses.

ACKNOWLEDGMENT

We thank Dr. Dean Edwards for constructs and Dr. David Toft for reagents. We also thank Dr. Carlos Catalano, Dr. N. Karl Maluf, and Keith Connaghan-Jones for critical input and helpful discussions.

REFERENCES

1. Tsai, M. J., and O'Malley, B. W. (1994) Molecular mechanisms of action of steroid/thyroid receptor superfamily members, *Annu. Rev. Biochem. 63*, 451−486.
2. Takimoto, G. S., Tung, L., Abdel-Hafiz, H., Abel, M. G., Sartorius, C. A., Richer, J. K., Jacobsen, B. M., Bain, D. L., and Horwitz, K. B. (2003) Functional properties of the N-terminal region of progesterone receptors and their mechanistic relationship to structure, *J. Steroid Biochem. Mol. Biol. 85*, 209−219.
3. Sartorius, C. A., Melville, M. Y., Hovland, A. R., Tung, L., Takimoto, G. S., and Horwitz, K. B. (1994) A third transactivation function (AF3) of human progesterone receptors located in the unique N-terminal segment of the B-isoform, *Mol. Endocrinol. 8*, 1347−1360.
4. Hurd, C., Nag, K., Khattree, N., Alban, P., Dinda, S., and Moudgil, V. K. (1999) Agonist and antagonist-induced qualitative and quantitative alterations of progesterone receptor from breast cancer cells, *Mol. Cell. Biochem. 199*, 49−56.
5. Conneely, O. M., Mulac-Jericevic, B., Lydon, J. P., and DeMayo, F. J. (2001) Reproductive functions of the progesterone receptor isoforms: lessons from knock-out mice, *Mol. Cell. Endocrinol. 179*, 97−103.
6. Shymala, G., Yang, X., Cardiff, R. D., Dale, E., Silberstein, G., and Barcellos-Hoff, M. H. (2000) Impact of progesterone receptor on cell-fate decisions during mammary gland development: Transgenic mice carrying an imbalance in the native ratio of A to B forms of progesterone receptor exhibit developmental abnormalities in mammary glands, *Proc. Natl. Acad. Sci. U.S.A. 97*, 3044−3049.
7. Richer, J. K., Jacobsen, B. M., Manning, N. G., Abel, M. G., Wolf, D. M., and Horwitz, K. B. (2002) Differential gene regulation by the two progesterone receptor isoforms in human breast cancer cells, *J. Biol. Chem. 277*, 5209−5218.
8. Hopp, T. A., Weiss, H. L., Hilsenbeck, S. G., Cui, Y., Alfred, D. C., Horwitz, K. B., and Fuqua, S. A. (2004) Breast cancer patients with progesterone receptor PR-A-Rich tumors have poorer disease-free survival rates, *Clin. Cancer Res. 15*, 2751−2760.
9. Liu, Z., Wong, J., Tsai, S. Y., Tsai, M.-J., and O'Malley, B. W. (2001) Sequential recruitment of steroid receptor coactivator-1 (SRC-1) and p300 enhances progesterone receptor-dependent initiation and reinitiation of transcription from chromatin, *Proc. Natl. Acad. Sci. U.S.A. 98*, 12426−12431.
10. Li, X., Wong, J., Tsai, S. Y., Tsai, M.-J., and O'Malley, B. W. (2003) Progesterone and glucocorticoid receptors recruit distinct coactivator complexes and promote distinct patters of local chromatin modification, *Mol. Cell. Biol. 23*, 3763−3773.
11. Arrowsmith, C. H., Carey, J., Treat-Clemons, L., and Jardetzky, O. (1989) NMR assignments for the amino-terminal residues of trp repressor and their role in DNA binding, *Biochemistry 28*, 3875−3879.
12. Johnson, A. D., Poteete, A. R., Lauer, G., Sauer, R. T., Ackers, G. K., and Ptashne, M. (1981) Lambda repressor and cro—components of an efficient molecular switch, *Nature 294*, 217−223.
13. Kumar, V., and Chambon, P. (1988) The estrogen receptor binds tightly to its responsive element as a ligand-induced homodimer, *Cell 55*, 145−156.
14. Drouin, J., Sun, Y. L., Tremblay, S., Lavender, P., Schmidt, T. J., de Lean, A., and Nemer, M. (1992) Homodimer formation is rate limiting for high affinity DNA binding by glucocorticoid receptor, *Mol. Endocrinol. 6*, 1299−1309.
15. DeMarzo, A. M., Beck, C. A., Onate, S. A., and Edwards, D. P. (1991) Dimerization of mammalian progesterone receptors occurs in the absence of DNA and is related to the release of the 90-kDa heat shock protein, *Proc. Natl. Acad. Sci. U.S.A. 88*, 72−76.
16. O'Malley, B. (1990) The steroid receptor superfamily: more excitement predicted for the future, *Mol. Endocrinol. 4*, 363−369.
17. Cohen-Solal, K., Bailly, A., Rauch, C., Quesne, M., and Milgrom, E. (1993) Specific binding of progesterone receptor to progesterone-responsive elements does not require prior dimerization, *Eur. J. Biochem. 214*, 189−195.
18. Skafar, D. F. (1991) Differential DNA binding by calf uterine estrogen and progesterone receptors results from differences in oligomeric state, *Biochemistry 30*, 6148−6154.
19. Rodriguez, R., Weigel, N. L., O'Malley, B., and Schrader, W. T. (1990) Dimerization of the chicken progesterone receptor in vitro can occur in the absence of hormone and DNA, *Mol. Endocrinol. 4*, 1782−1790.
20. Jacobsen, B. M., Richer, J. K., Schittone, S. A., and Horwitz, K. B. (2002) New human breast cancer cells to study progesterone receptor isoform ratio effects and ligand-independent gene regulation, *J. Biol. Chem. 277*, 27793−27800.
21. Jacobsen, B. M., Schittone, S. A., Richer, J. K., and Horwitz, K. B. (2005) Progesterone-independent effects of human progesterone receptors (PR) in estrogen receptor-positive breast cancer: PR isoform-specific gene regulation and tumor biology, *Mol. Endocrinol. 19*, 574−587.
22. Metivier, R., Penot, G., Hubner, M. R., Reid, G., Brand, H., Kos, M., and Gannon, F. (2003) Estrogen receptor-alpha directs ordered, cyclical, and combinatorial recruitment of cofactors on a natural target promoter, *Cell 115*, 751−763.
23. Nagaich, A. K., Walker, D. A., Wolford, R., and Hager, G. L. (2004) Rapid periodic binding and displacement of the glucocorticoid receptor during chromatin remodeling, *Mol. Cell 14*, 163−174.
24. Christensen, K., Estes, P. A., Onate, S. A., Beck, C. A., DeMarzo, A., Altmann, M., Lieberman, B. A., St. John, J., Nordeen, S. K., and Edwards, D. P. (1991) Characterization and functional properties of the A and B forms of human progesterone receptors synthesized in a baculovirus system, *Mol. Endocrinol. 5*, 1755−1770.
25. Tetel, M. J., Jung, S., Carbajo, P., Ladtkow, T., Skafar, D. F., and Edwards, D. P. (1998) Hinge and amino-terminal sequences contribute to solution dimerization of human progesterone receptor, *Mol. Endocrinol. 11*, 1114−1128.
26. Gill, S., and von Hippel, P. (1989) Calculation of protein extinction coefficients from amino acid sequence data, *Anal. Biochem. 182*, 319−326.
27. Edelhoch, H. (1967) Spectroscopic determination of tryptophan and tyrosine in proteins, *Biochemistry 6*, 1948−1954.
28. Pace, C. N., Vajdos, F., Fee, L., Grimsley, G., and Gray, T. (1995) How to measure and predict the molar absorption coefficient of a protein, *Protein Sci. 4*, 2411−2423.

29. Lakowicz, J. R. (1983) *Principles of Fluorescence*, Plenum Press, New York.
30. Stafford, W. F. (1992) Boundary analysis in sedimentation transport experiments: A procedure for obtaining sedimentation coefficient distributions using the time derivative of the concentration profile, *Anal. Biochem. 203*, 295−301.
31. Van Holde, K. E. (1971) *Physical Biochemistry*, Prentice-Hall, Englewood Cliffs, CA.
32. Waxman, E., Laws, W. R., Laue, T. M., Nemerson, Y., and Ross, J. B. A. (1993) Human factor VIIa and its complex with soluble tissue factor: evaluation of symmetry and conformational dynamics by ultracentrifugation and fluorescence anisotropy decay methods, *Biochemistry 32*, 3005−3012.
33. Passen, H., and Kumosinski, T. F. (1985) Measurements of protein hydration by various techniques, *Methods Enzymol. 117*, 219−255.
34. Laue, T. M., Shah, B. D., Ridgeway, T. M., and Pelletier, S. L. (1992) *Analytical Ultracentrifugation in Biochemistry and Polymer Science*, Royal Society of Chemistry, Cambridge.
35. Cohn, E. J., and Edsall, J. T. (1943) *Proteins, Amino Acids and Peptides*, Reinhold, New York.
36. Johnson, M. L., Correia, J. J., Yphantis, D. A., and Halvorson, H. R. (1981) Analysis of data from the analytical ultracentrifuge by nonlinear least-squares techniques, *Biophys. J. 36*, 575−588.
37. Maluf, N. K., and Lohman, T. M. (2003) Self-association equilibria of *E. coli* UvrD helicase studied by analytical ultracentrifugation, *J. Mol. Biol. 325*, 889−912.
38. Smith, D. F., Lubahn, D. B., McCormick, D. J., Wilson, E. M., and Toft, D. O. (1988) The production of antibodies against the conserved cysteine region of steroid receptors and their use in characterizing the avian progesterone receptor, *Endocrinology 122*, 2816−2825.
39. Goel, A., Colcher, D., and Koo, J. S. (2000) Relative position of the hexahistidine tag effects binding properties of a tumor-associated single-chain Fv construct, *Biochim. Biophys. Acta 1523*, 13−20.
40. Bain, D. L., Franden, M. A., McManaman, J. L., Takimoto, G. S., and Horwitz, K. B. (2000) The N-terminal region of the human progesterone A-receptor: Structural analysis and the influence of the DNA binding domain, *J. Biol. Chem. 275*, 7313−7320.
41. Bain, D. L., Franden, M. A., McManaman, J. L., Takimoto, G. S., and Horwitz, K. B. (2001) The N-terminal region of human progesterone B-receptors: biophysical and biochemical comparison to A-receptors, *J. Biol. Chem. 276*, 23825−23831.
42. Schrader, W. T. (1975) Methods for extraction and quantification of receptors, *Methods Enzymol. 36*, 187−211.
43. Chen, Z., Shemshedini, L., Durand, B., Noy, N., Chambon, P., and Gronemeyer, H. (1994) Pure and functionally homogeneous recombinant retinoid X receptor, *J. Biol. Chem. 269*, 25770−25776.
44. Edwards, D. P., Altmann, M., DeMarzo, A., Zhang, Y., Weigel, N. L., and Beck, C. A. (1995) Progesterone receptor and the mechanism of action of progesterone antagonists, *J. Steroid Biochem. Mol. Biol. 53*, 449−458.
45. El-Ashry, D., Onate, S. O., Nordeen, S., and Edwards, D. P. (1989) Human progesterone receptor complexed with the antagonist RU486 binds to hormone response elements in a structurally altered form, *Mol. Endocrinol. 3*, 1545−1558.
46. Meyer, M. E., Pornon, A., Ji, J. W., Bocquel, M. T., Chambon, P., and Gronemeyer, H. (1990) Agonistic and antagonistic activities of RU486 on the functions of the human progesterone receptor, *EMBO J. 9*, 3923−3932.
47. Hurd, C., and Moudgil, V. K. (1988) Characterization of R5020 and RU486 binding to progesterone receptor from calf uterus, *Biochemistry 27*, 3618−3623.
48. Kastner, P., Krust, A., Turcotte, B., Stropp, U., Tora, L., Gronemeyer, H., and Chambon, P. (1990) Two distinct estrogen-regulated promoters generate transcripts encoding the two functionally different human progesterone receptor forms A and B, *EMBO J. 9*, 1603−1614.
49. Philo, J. S., Yang, T. H., and LaBarre, M. (2004) Re-examining the oligomerization state of macrophage migration inhibitory factor (MIF) in solution, *Biophys. Chem. 108*, 77−87.
50. Wong, I., and Lohman, T. M. (1995) Linkage of protein assembly to protein-DNA binding, *Methods Enzymol. 259*, 95−127.
51. Williams, S. P., and Sigler, P. B. (1998) Atomic structure of progesterone complexed with its receptor, *Nature 393*, 392−396.
52. Tanmrazi, A., Carlson, K. E., Daniels, J. R., Hurth, K. M., and Katzenellenbogen, J. A. (2002) Estrogen receptor dimerization: ligand binding regulates dimer affinity and dimer dissociation rate, *Mol. Endocrinol. 16*, 2706.
53. Shiau, A. K., Barstad, D., Loria, P. M., Cheng, L., Kushner, P. J., Agard, D. A., and Greene, G. L. (1998) The structural basis of estrogen receptor/coactivator recognition and the antagonism of this interaction by tamoxifen, *Cell 95*, 927−937.
54. Pratt, W. B., and Toft, D. O. (1997) Steroid receptor interactions with heat shock protein and immunophilin chaperones, *Endocrine Rev. 18*, 306−360.
55. Wyman, J. (1964) Linked functions and reciprocal effects in hemoglobin: a second look, *Adv. Protein Chem. 19*, 223−286.
56. Prendergast, P., Onate, S. A., Christensen, K., and Edwards, D. P. (1994) Nuclear accessory factors enhance the binding of progesterone receptor to specific target DNA, *J. Steroid Biochem. Mol. Biol. 48*, 1−13.
57. Theofan, G., and Notides, A. C. (1984) Characterization of the calf uterine progesterone receptor and its stabilization by nucleic acids, *Endocrinology 114*, 1173−1179.
58. Segard-Maurel, I., Rajkowski, K., Jibard, N., Schweizer-Groyer, G., Baulieu, E.-E., and Cadepond, F. (1996) Glucocorticoid receptor dimerization investigated by analysis of receptor binding to glucocorticosteroid responsive elements using a monomer−dimer equilibrium model, *Biochemistry 35*, 1634−1642.
59. Perlmann, T., Eriksson, P., and Wrange, O. (1990) Quantitative analysis of the glucocorticoid receptor-DNA interaction at the mouse mammary tumor virus glucocorticoid response element, *J. Biol. Chem. 265*, 17222−17229.
60. Liao, M., Zhou, Z.-x., and Wilson, E. M. (1999) Redox-dependent DNA binding of the purified androgen receptor: evidence for disulfide-linked androgen receptor dimers, *Biochemistry 38*, 9718−9727.
61. Wrange, O., Carlstedt-Duke, J., and Gustafsson, J.-A. (1986) Stoichiometric analysis of the specific interaction of the glucocorticoid receptor with DNA, *J. Biol. Chem. 261*, 11770−11778.

BI050609I